

# A Non-Convex Control Allocation Strategy as Energy-Efficient Torque Distributors for On-Road and Off-Road Vehicles

A. M. Dizqah<sup>a,\*</sup>, B. L. Ballard<sup>b</sup>, M. V. Blundell<sup>b</sup>, S. Kanarachos<sup>b</sup>, M. S. Innocente<sup>b</sup>

<sup>a</sup>*Smart Vehicles Control Laboratory (SVeCLab), University of Sussex, Brighton, BN1 9QT, UK*

<sup>b</sup>*Institute for Future Transport and Cities, Coventry University, Coventry, CV1 2TT, UK*

---

## Abstract

Vehicles with multiple drivetrains, like hybrid electric powertrains, are over-actuated systems with an infinite number of feasible solutions that fulfil primary objectives such as providing the total torque demand by individual contribution of multiple drivetrains. Hence, energy efficiency is considered as the secondary objective to determine the optimum solution. However, the resulting optimisation problem, which is nonlinear due to multi-modal operation of electric machines, must be solved very quickly to comply with stability requirements of vehicle dynamics. A theorem is developed for the first time to formulate and parametrically solve the energy-efficient torque distribution problem for vehicles with multiple different drivetrains. The parametric solution is deployable on ordinary electronic control units (ECUs) as a small-size lookup table that makes it very fast in operation. The traction efficiency of the off-road conditions is formally integrated into the developed theorem to be considered in the provided torque distribution strategies. Simulation results indicate effectiveness of the provided optimal solution as energy management strategies for on-road and off-road electrified vehicles with multiple different drivetrains.

**Keywords:** Traction Efficiency, Control Allocation, Energy Management Strategies, Hybrid Electric Vehicles, Power Loss, Multiple Drivetrains

---

## 1. Introduction

Traditionally, vehicles consist of conventional drivetrains with a single internal combustion Diesel or petrol engine. Electrification, on the other hand, introduces additional electric drivetrain to the vehicle powertrain. Also, fully-electric vehicles can consist of multiple drivetrains, instead of only one, making them suitable to employ the safety and drivability control strategies like torque-vectoring Dizqah et al. (2016). Thus, modern powertrains are over-actuated systems which can provide desired traction torques and yaw moments with an infinite number of feasible contributions of their multiple drivetrains. This makes it possible to dynamically find an optimum set of the drivetrains contribution in terms of a secondary objective like minimising energy consumption.

It is shown in Dizqah et al. (2016); Suzuki et al. (2014) that energy efficiency can be improved by optimal torque distribution among multiple drivetrains. The authors in Chen and Wang (2014a,b) presented a torque distribution strategy (TDSs) based on minimising power dissipation of drivetrains and showed the superior performance of their strategy comparing to simple even distribution. Their strategy is effective however it does not take the

effects of variation of vehicle parameters, like speed, into account.

The authors in Dizqah et al. (2016) introduced a solution to the parametric torque distribution problem that is calculated off-line to optimally, in terms of energy consumption, distribute total torque demands among multiple electric drivetrains. The developed solution is implemented on an electronic control unit (ECU) as a small-sized lookup table that results in high-speed computation. They showed that applying their developed control strategy reduces energy consumption up to 4.6% subject to driving cycles.

The developed strategy uses the power loss curve of drivetrains and takes the vehicle speed into account as a parameter. The power loss of a drivetrain includes all the losses from tank or battery to tyre (or the other way around for regenerative function), considering thermal, mechanical and electrical efficiencies and resistances. The losses are measured in terms of actual torque at the contact patch of tyres at different vehicle speeds and the results are illustrated as a parametric curve like the one in Figure 1a Dizqah et al. (2016). These parametric curves are called power loss curves and are measured using rolling road test benches like the one in Figure 1b Dizqah et al. (2016).

The authors in Dizqah et al. (2016) assumed that drivetrains are the same with reference to their power loss curves which are monotonically increasing in terms of torque

---

\*Corresponding author

Email address: [am2114@sussex.ac.uk](mailto:am2114@sussex.ac.uk) (A. M. Dizqah)

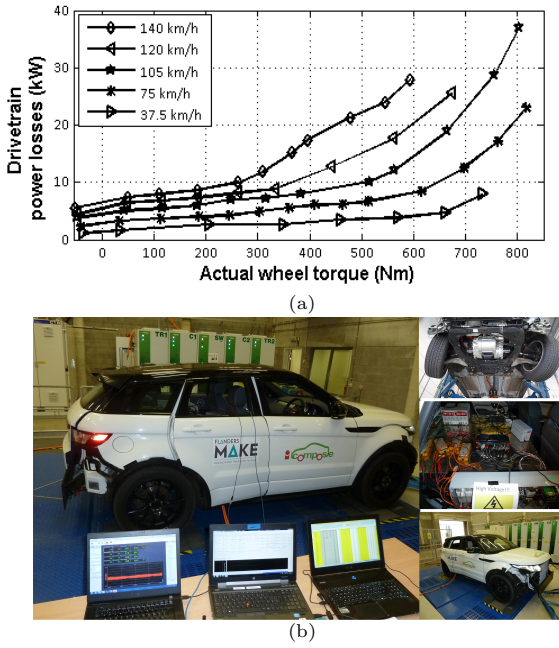


Figure 1: (a) Example of power loss curves, in terms of wheel torques at different vehicle speeds, measured using (b) a sample of rolling road test bench introduced in Dizqah et al. (2016)

demand. However, it is already shown in Tang (2010) that employing multiple electric drivetrains with different power loss curves improves the overall efficiency further. Moreover, hybrid electric powertrains are not addressable by Dizqah et al. (2016) because the conventional and electric drivetrains are different in their characteristics such as power loss and maximum torque curves.

The authors in Lenzo et al. (2017) expanded the introduced theorem in Dizqah et al. (2016) to cover cases when power loss curves are different due to load transformation. The load transformation happens during vehicle acceleration and deceleration when the normal loads on the tyres and therefore the tyres parameters change. The introduced extension is effective, however, it is based on two main assumptions: i) the power loss curves are monotonically increasing; and ii) the power loss curves are well matched to a third-order polynomial. These assumptions prevents the strategies from being useful to realistic applications like off-road vehicles and hybrid electric powertrains.

Neither Lenzo et al. (2017) nor Dizqah et al. (2016) deal with the torque distribution problem of off-road vehicles. With on-road conditions, traction efficiency of tyres (i.e. the ratio of the generated drawbar thrust power to the applied driving power) are quite high and negligible in design of torque distribution strategies. Unlike the on-road conditions, the traction efficiency of tyres play a major role in off-road vehicles where the resistance to motion is much higher and substantially dominated by the terrain type and sinkage of tyres into soil Senatore and Sandu (2011a); Vantsevich (2007); Taheri et al. (2015). The sinkage sharply decreases, and hence the traction ef-

iciency increases, by compacting the soil due to multiple passes of tyres over the same traveling track. This phenomenon is called multi-pass effect. Traction efficiency of the front and rear wheels of four-wheel off-road vehicles are significantly different particularly for the first passes where front wheel compacts the soil ahead of rear wheel.

The authors in Vantsevich (2007); Senatore and Sandu (2011b) investigated the impact of torque distribution strategies on the traction efficiency of off-road vehicles. They have analytically shown that the traction efficiency is maximised when the slip ratio of front and rear tyres are the same. The slip ratio is the normalised difference between rotational and longitudinal speeds of tyres as a measure of their slippage. The authors in Vantsevich (2007); Senatore and Sandu (2011b) indicated that their claim is only valid if both front and rear tyres operate exactly in the same way which is not usually the case due to load transformation and the multi-pass effect amongst others. It is also shown in Dizqah et al. (2016) that such even distribution strategy is only applicable to drivetrains with convex power loss curves which is not valid most of the time.

Energy management strategies (EMSs) of hybrid electric vehicles (HEVs) optimally split, comparable to TDSs, the power demands between multiple energy sources in terms of objectives like minimising energy consumption. The authors in Huang et al. (2018) provided a comprehensive review of EMSs for HEVs indicating that majority of the recent researches in this area focused on formulating and solving the strategies as model-predictive controllers. However, such formulation is applicable to either of two cases: i) off-line calculation of the optimum distribution as benchmark for a priori known driving cycle with boundary conditions on state-of-charge of batteries Huang et al. (2018); or ii) on-line management of the hybrid electrical storage systems consisting of fast components like supercapacitors. The response time of batteries, as potentially the only electrical storage of HEVs, are significantly larger than prediction horizon of on-line controllers, and hence negligible in design of the controllers. The prediction horizon, on the other hand, is a short future time that the vehicle speed is predicted for and fed into on-line EMSs.

Unlike EMSs which are majorly slow controllers managing energy storage systems, TDSs are faster due to vehicle dynamics requirements and manage instantaneous contributions of multiple drivetrains. The authors in Wang et al. (2018) proposed an energy management strategy for off-road vehicles with series hybrid electric powertrain and hybrid energy storage. They have developed a model-predictive control strategy to minimise fuel consumption and regulate the state of charge of battery and supercapacitor packs to certain values. The simulation results in Wang et al. (2018) show that using a hybrid battery-supercapacitor storage reduces cost, weight and volume of an off-road bulldozer while providing a comparable efficiency in terms of fuel consumption. However, the paper does not answer the question: How does an optimal torque

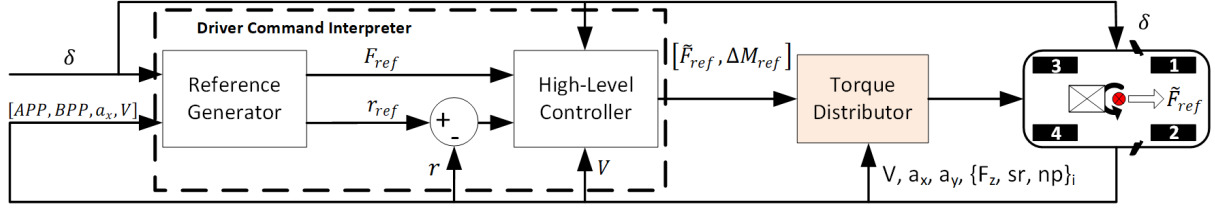


Figure 2: The vehicle dynamics control structure with the proposed torque distribution block. In case of off-road vehicles, the normal load  $F_z$ , slip ratio  $sr$  and number of passes  $np$  are also fed into the developed torque distribution strategy

distribution between the multiple electric drivetrains of the bulldozer impacts energy consumption?.

This paper addresses the above mentioned gaps through the following novel contributions to the knowledge:

- Energy-efficient torque distribution between different drivetrains of a vehicle is formulated as a unified non-convex problem. A theorem is proposed for the first time to convert the resulting non-convex problem to a quadratic programming (QP) problem, solvable offline to be stored as small-sized lookup tables in ECU. Unlike Dizqah et al. (2016); Lenzo et al. (2017); Vantsevich (2007); Senatore and Sandu (2011b), the proposed theorem is not restricted to the drivetrains with the same monotonically increasing power loss curves. The effects of load transformation due to lateral and longitudinal accelerations are also integrated into the developed theorem and the solution efficacy has been proven.
- The introduced theorem is used to develop a novel torque distribution strategy for off-road vehicles with multiple electric drivetrains, shown to be more effective in reducing energy consumption compared to prior reported strategies.
- The theorem is also applied as offline solution for the optimal torque distribution problem of compound hybrid powertrains without supercapacitors.

The remainder of this paper is organised as follows: Section 2 formulates the problem mathematically as a multi-parametric programming problem. The developed theory is introduced in Section 3, including all details of the introduced control strategy. Section 4 provides all simulation results for on-road and off-road case studies and verifies the effectiveness of the introduced control strategy. The paper is concluded in Section 5.

## 2. Problem Statement and Formulation

Fig. 2 shows a simplified version of the vehicle control hierarchy including the proposed torque distribution block for the on-road and off-road vehicles. Reference yaw rate,  $r_{ref}$ , and total required traction/braking force,  $F_{ref}$  is produced by a reference generator having steering wheel angle ( $\delta$ ), accelerator and brake pedal positions

(respectively  $APP$  and  $BPP$ ), as well as the longitudinal vehicle speed and acceleration (respectively  $V$  and  $a_x$ ). Then, the high-level controller overrides longitudinal force, if required, and determines the modified reference of traction force,  $\tilde{F}_{ref}$ , alongside the additional yaw moment  $\Delta M_{ref}$  required for stability and safety purposes. The proposed torque distribution algorithm, as a multi-parametric control allocation strategy, then minimises the powertrain power losses as a secondary objective while maintaining  $\tilde{F}_{ref}$  and  $\Delta M_{ref}$  as the primary objective. The algorithm takes multiple parameters into account: vehicle's speed and accelerations; as well as normal load ( $F_z$ ) and number of passes ( $np$ ) of tyres.

The number of passes ( $np$ ) indicates the number of travels already occurred over the same track and is a measure of soil compactness due to the multi-pass effect. It is zero or a positive number however the first and second passes changes sinkage of the tyres into the soil much more than the next passes because the soil under the tyres become such compact that does not change significantly with more passes Senatore and Sandu (2011a); Vantsevich (2007); Taheri et al. (2015). In four-wheel off-road vehicles, where the rear wheel mostly travels on the same track that already passed by the front wheel,  $np = m : n$  where  $m$  and  $n$  are respectively numbers of already occurred passes of the front and rear tyres and  $n = m + 1$ . For instance,  $np = 0 : 1$  says that there is no prior pass over the soil under front tyre though rear tyre travels over the track already compressed by the front tyre.

The authors in Dizqah et al. (2016) showed that the optimal torque distribution problem among multiple different drivetrains is a nonlinear multiparametric programming problem (mp-NLP). The mp-NLP problems are broadly formulated as follows Domínguez et al. (2010); Grancharova and Johansen (2012):

$$z^*(\theta) = \underset{\mathbf{T}_w \in \Theta}{\text{minimise}} \quad J(\mathbf{T}_w; \theta) \quad (1a)$$

$$s.t. \quad G(\mathbf{T}_w; \theta) \leq 0; \quad (1b)$$

$$H(\mathbf{T}_w; \theta) = 0; \quad (1c)$$

$$\theta \in \Theta \quad (1d)$$

where  $\Theta$  is the feasible set of the parameter vectors  $\theta$ , and  $G$  and  $H$  represent the inequality and equality constraints.  $J$  is the cost function which depends on the set of traction and generation torques (which are alphabetised by respectively  $t$  and  $g$  hereafter) of each wheel's drivetrain as the decision variables  $\mathbf{T}_w = [\tau_{w,t_{FL}} \ \tau_{w,t_{FR}} \ \tau_{w,t_{RL}} \ \tau_{w,t_{RR}} \ \tau_{w,g_{FL}} \ \tau_{w,g_{FR}} \ \tau_{w,g_{RL}} \ \tau_{w,g_{RR}}]$

$\in T; \tau_{w,t_i}, \tau_{w,g_i} \geq 0 \quad i \in \{FL, FR, RL, RR\}$  (F: front, R: Rear, L:left, R:right), as well as on the parameters  $\theta \in \Theta$ .  $T$  represents the feasible set of decision variables. It is important to note that since the problem depends on parameters  $\theta$ , the optimal decision variables  $\mathbf{T}_w^*(\theta)$  and the corresponding optimal value  $z^*(\theta)$  are also parametric. In other words, the optimal solution changes with respect to the value of parameters  $\theta$ .

The cost function  $J(\mathbf{T}_w; \theta)$  is defined as the total energy consumption of the powertrain, which is the difference between the sum of the total traction power and the sum of the total regenerated powers of all wheels. It is shown in Dizqah et al. (2016) that such a cost function is equivalent to:

$$J(\mathbf{T}_w; \theta) = \sum_{i \in \{FL, FR, RL, RR\}} [P_{loss,t_i}(\tau_{w,t_i}; \theta) - P_{loss,g_i}(\tau_{w,g_i}; \theta)] \quad (2)$$

which only depends on the power loss of the traction ( $P_{loss,t_i}$ ) and regeneration ( $P_{loss,g_i}$ ) modes of each wheel. It is worth noting that the sign of the traction and regeneration powers are different since unlike the traction power which is discharged from the battery, the regenerated power is stored.

In effect, the optimal torque distribution problem of a vehicle with four drivetrains, one per wheel, for small steering angles is formulated as follows Dizqah et al. (2016):

$$\mathbf{T}_w^*(\theta) = \arg \min_{\mathbf{T}_w \in T} J(\mathbf{T}_w; \theta) \quad (3a)$$

$$:= \sum_i [P_{loss,t_i}(\tau_{w,t_i}; \theta) - P_{loss,g_i}(\tau_{w,g_i}; \theta)]$$

$$s.t. \quad A\mathbf{T}_w = R_{eff}[\theta_1, \theta_2]^T; \quad (3b)$$

$$0 \leq \tau_{w,t_i} \leq \tau_{w,t_{max}}(\theta); \quad (3c)$$

$$0 \leq \tau_{w,g_i} \leq \tau_{w,g_{max}}(\theta); \quad (3d)$$

$$\tau_{w,t_i} \tau_{w,g_i} = 0; \quad (3e)$$

$$\theta_{min} \leq \theta \leq \theta_{max} \quad (3f)$$

$$i \in \{FL, FR, RL, RR\}.$$

where  $R_{eff}$  is the effective radius of tyres and it is assumed that the vehicle operates within a limited range of yaw rates.  $A$  is defined as follows:

$$A = \begin{bmatrix} 1 & 1 & 1 & 1 & -1 & -1 & -1 & -1 \\ -d & d & -d & d & d & -d & d & -d \end{bmatrix} \quad (4)$$

where  $d$  is the front and rear half-track.

The  $\theta_{1 \times n}$  is a  $n$ -dimensional vector where  $n$  is the number of parameters. The first two parameters are: the reference longitudinal force ( $\theta_1 = \tilde{F}_{ref}$ ); and the desired yaw moment to be generated by unequal torque distribution among wheels ( $\theta_2 = \Delta M_{ref}$ ). The other parameters like vehicle speed or number of passes are selected as per application in section IV.

The first row of (3b) formulates the fact that the sum of tractive minus regenerative torques is the same as the desired total torque of  $\tilde{F}_{ref} R_{eff}$ . The second row indicates

that the generated yaw moment, due to unequal torques applied to the left- and right-side of vehicle, is the same as the reference value of  $\Delta M_{ref}$ .

Problem (3) is a non-convex optimisation problem due to the complementarity constraint  $\tau_{w,i,t} \tau_{w,i,g} = 0; \tau_{w,i,t} \tau_{w,i,g} \geq 0$  which formulates the fact that each wheel only operates in traction or regeneration at each moment. Moreover, power loss curves of  $P_{loss,t_i}$  and  $P_{loss,g_i}$  in (3a) are non-convex Dizqah et al. (2016).

### 3. Design of Control Strategy

It is already shown in Dizqah et al. (2016) that holding the following assumption:

**Assumption 1.** The vehicle consists of four identical electric drivetrains which have equal power loss characteristics, i.e.,  $P_{loss}(\tau_w; \theta) = P_{loss,t/g_i}(\tau_{w,t/g_i}; \theta); i \in \{FL, FR, RL, RR\}$  holding for either traction or regeneration.

problem (3) can be split into two separate problems as per left- and right-side of the vehicle. The resulting problem per each side is as follows:

$$\begin{aligned} \{\tau_{w_F}, \tau_{w_R}\}^*(\tau_w^*, \theta) &= \arg \min_{\tau_{w_F}, \tau_{w_R} \in T} J(\tau_{w_F}, \tau_{w_R}; \theta) \\ &:= P_{loss_F}(\tau_{w_F}; \theta) + P_{loss_R}(\tau_{w_R}; \theta) \end{aligned} \quad (5a)$$

$$s.t. \quad B[\tau_{w_F}, \tau_{w_R}]^T = R_{eff} \tau_w^*; \quad (5b)$$

$$0 \leq \tau_{w_F}, \tau_{w_R} \leq \tau_{w_{max}}(\theta). \quad (5c)$$

where  $B$  is defined as one of the following values depending on the traction and regeneration modes of tyres:

$$[1 \quad 1]; [1 \quad -1]; [-1 \quad 1] \quad (6)$$

and  $\tau_w^*$  is the total side torque at contact patches of wheels which is calculated using the following Lemma Dizqah et al. (2016):

**Lemma 1.** Meeting equality constraints of problem (3), there is only one feasible set of values for the total torque of vehicle sides which is calculated as follows:

$$\tau_{w,l}^* = 0.5 \left( \tilde{F}_{ref} - \frac{\Delta M_{ref}}{d} \right) R_{eff}; \quad (7a)$$

$$\tau_{w,r}^* = 0.5 \left( \tilde{F}_{ref} + \frac{\Delta M_{ref}}{d} \right) R_{eff}. \quad (7b)$$

where  $\tau_{w,l}^*$  and  $\tau_{w,r}^*$  are, respectively, the reference total torques of the left- and right-hand sides of the vehicle.

Also, holding the following assumption:

**Assumption 2.** The drivetrain power loss curve of each corner of vehicle is positive and monotonically increasing in terms of the torque demand,  $\tau_w$ . In other words, both the  $P_{loss,t/g_i}(\tau_{w,t/g_i}; \theta) \geq 0$  and  $\partial P_{loss,t/g_i}(\tau_{w,t/g_i}; \theta) / \partial \tau_{w,t/g_i} \geq 0$  are met.



the authors in Dizqah et al. (2016) proved that:

**Lemma 2.** If Assumptions 2 hold, the optimal torque distributions make both front and rear drivetrains of each side of the vehicle work in either traction or regeneration.

Consequently, the solution of (3) is calculated by simultaneously solving of (5) for both left- and right-side of vehicle. The optimum solution of (5) for each side is either applying total torque to a single wheel (axle) or evenly distributing the total torque between the front and rear wheels Dizqah et al. (2016). The optimum switching points between these two cases depend on the vehicle parameters and are calculated as follows Dizqah et al. (2016):

**Theorem 1.** Holding Assumptions 1 and 2, the optimal solution of each side of the vehicle is:

- Single-axle, for small values of the reference torque demand;
- Even distribution among the wheels, for large values of the reference torque demand;
- And the optimal switching point between strategies (a) and (b) at each value of  $\theta = \theta_0$  is calculated as the solution of:

$$P_{loss}(\tau_{sw}; \theta_0) + P_{loss}(0; \theta_0) = 2P_{loss}(0.5\tau_{sw}; \theta_0). \quad (8)$$

where  $\tau_{sw}$  is the torque, named as switching torque, at which the controller switches between the single-axle and even distribution strategies.

However, as described in Section I, these two assumptions are not held for most real cases. For instance, the power loss curves of the wheels of off-road vehicles are different due to the multi-pass effect, regardless the similarity or non-similarity of the drivetrains. Moreover, the drivetrains composing hybrid electric powertrains are intuitively different in terms of technologies, efficiency maps and therefore power loss curves. Furthermore, vehicle accelerations cause variations of normal loads on the tyres making the power loss curves of each drivetrain different and hence failing Assumption 1.

To address the above mentioned issues, Theorem 2 is introduced in this paper as below to formulate and prove a general tool to develop energy-efficient torque distribution strategies for the on-road and off-road vehicles with multiple drivetrains.

**Theorem 2.** The solution of (5) and hence the optimum torques applied to the front and rear wheels of vehicles with multiple drivetrains are:

$$\tau_{w_f}^* = \tau_0 + \epsilon^*; \quad (9a)$$

$$\tau_{w_r}^* = \tau_0 - \epsilon^*. \quad (9b)$$

where  $\tau_0 = 0.5 \times \tilde{F}_{ref} \times R_{eff}$  is half of the total torque demand per vehicle side (i.e., the even-distribution solution)

and  $\epsilon^*$  is the optimum deviation from the even distribution. Then,  $\epsilon^*$  is the solution of the following quadratic optimization problem at any given value of parameters  $\theta = \theta_0$ :

$$\epsilon^*(\tau_0; \theta_0) = \arg \underset{\epsilon}{\text{minimise}} J(\epsilon; \tau_0, \theta_0) := \quad (10a)$$

$$\begin{aligned} & \frac{1}{2}(\nabla_{\tau\tau}^2 P_{loss,f}(\tau; \theta_0)|_{\tau=\tau_0} + \\ & \nabla_{\tau\tau}^2 P_{loss,r}(\tau; \theta_0)|_{\tau=\tau_0}) \epsilon^2 + \\ & (\nabla_{\tau} P_{loss,f}(\tau; \theta_0)|_{\tau=\tau_0}) - \\ & \nabla_{\tau} P_{loss,r}(\tau; \theta_0)|_{\tau=\tau_0}) \epsilon + \\ & s.t. \quad -\tau_0 \leq \epsilon \leq \tau_0. \end{aligned} \quad (10b)$$

*Proof.* The optimal distribution of the total torque demand of  $\tau_w$  for each side of the vehicle is the solution of (5). By approximating the cost function of (5) around  $\tau_0$ , the resulting Taylor series is:

$$\begin{aligned} J(\tau_{w_f}, \tau_{w_r}; \theta_0) & \cong P_{loss_f}(\tau_0; \theta_0) + \nabla_{\tau} P_{loss_f}(\tau_0; \theta_0)(\tau_{w_f} - \tau_0) + \\ & \frac{1}{2} \nabla_{\tau\tau}^2 P_{loss_f}(\tau_0; \theta_0)(\tau_{w_f} - \tau_0)^2 + \\ & P_{loss_r}(\tau_0; \theta_0) + \nabla_{\tau} P_{loss_r}(\tau_0; \theta_0)(\tau_{w_r} - \tau_0) + \\ & \frac{1}{2} \nabla_{\tau\tau}^2 P_{loss_r}(\tau_0; \theta_0)(\tau_{w_r} - \tau_0)^2. \end{aligned} \quad (11)$$

Substituting (9) into (11), one reformulates (11) as follows:

$$\begin{aligned} J(\epsilon; \tau_0, \theta_0) & \cong \overbrace{P_{loss_f}(\tau_0; \theta_0) + P_{loss_r}(\tau_0; \theta_0)}^{\text{Total losses by even distribution}} + \\ & (\nabla_{\tau} P_{loss_f}(\tau; \theta_0)|_{\tau=\tau_0} - \nabla_{\tau} P_{loss_r}(\tau; \theta_0)|_{\tau=\tau_0}) \epsilon + \\ & \frac{1}{2}(\nabla_{\tau\tau}^2 P_{loss_f}(\tau; \theta_0)|_{\tau=\tau_0} + \nabla_{\tau\tau}^2 P_{loss_r}(\tau; \theta_0)|_{\tau=\tau_0}) \epsilon^2. \end{aligned} \quad (12)$$

The first two terms are constant and positive for each pair of  $(\tau_0; \theta)$  and therefore the cost function (12) is minimised by solving (10) and choosing the optimum value  $\epsilon^*$ .

Constraints (10b) implies that the front and rear torques must be within  $[0, 2\tau_0]$ . Depending on the engaged drivetrains, other boxing constraints may also be added.

If the power loss curves are not locally monotonically-increasing in terms of the torque demand, (5) must be solved for all values of matrix  $B$  and the one with the minimum power loss is selected.  $\square$

**Remark 1.** The higher order derivatives can also be added to the Taylor expansion in (11) for power loss curves with large Lipschitz constant (i.e. stiffer functions), leading to a non-linear optimization problem; however, for normal power loss curves the coefficients of the higher order terms are small and therefore the higher order derivatives of the Taylor expansion are negligible.

**Remark 2.** Problem (10) is solved online using a quadratic programming tool for different values of  $B$  and instantaneous values of torque demand and parameters. Alternatively, it can be solved offline as a mp-NLP Domínguez et al. (2010); Grancharova and Johansen (2012) and the solution is stored in ECU as a look up table.

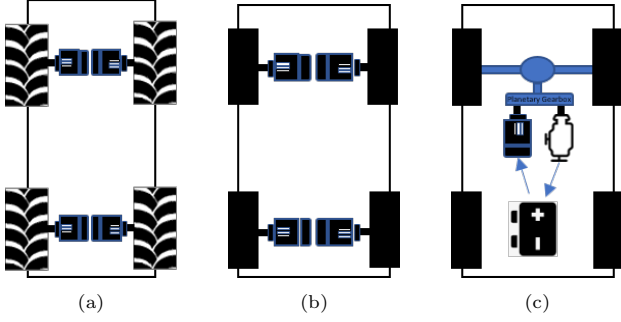


Figure 3: Powertrain layouts of studied vehicles: (a) Off-Road with four independent per-wheel drivetrains; (b) Electric powertrain with four independent per-wheel drivetrains; and (c) Compound hybrid electric powertrain with batteries as electric storage.

**Remark 3.** If for any torque demand  $\tilde{F}_{ref} \cdot R_{eff}$  the difference of the gradient and the sum of the hessian of power losses at  $\tau_0$  are both zero, then even distribution is the optimum solution.

**Remark 4.** If the difference of the gradient and the sum of the hessian of power losses at  $\tau_0$  are both negative, then  $\epsilon = \tau_0$  is the optimum solution of (10) and hence single-axle is the optimum solution.

#### 4. Case Studies and Simulation Results

The effectiveness of the developed Theorem is investigated through design and analysis of three torque distributors for vehicles in Figure 3. First, Theorem 2 is used to develop an energy-efficient torque distributor for off-road vehicles by taking both the drivetrains' and traction efficiencies into account. The traction efficiencies are calculated using the experimental results provided in Vantsevich (2007); Senatore and Sandu (2011a). Second, the developed theorem is used to extend the introduced controller in Dizqah et al. (2016) to electric vehicles with multiple drivetrains travelling with lateral and longitudinal accelerations. Finally, an optimal energy management strategy is developed to minimise total energy consumption of compound hybrid electric powertrains with batteries as the only electric storage.

On-road simulations have been conducted using the SIMULINK Toolbox of Vehicle Dynamics. The analysis and simulation results indicate all three developed controllers are optimal in terms of energy consumption.

##### 4.1. Optimal TDS for Off-Road Vehicles

In contrast to on-road vehicles where the traction efficiencies are negligible, the efficiencies are considerable for off-road applications. Hence the power loss of each drivetrain of off-road vehicles, from energy source to the resulting force at drawbar, is calculated as follows:

$$P_{loss}(\theta') = \left( \frac{1}{\eta_{dr}(\theta')\eta_t(\theta')} - 1 \right) F_x(\theta') V_x. \quad (13)$$

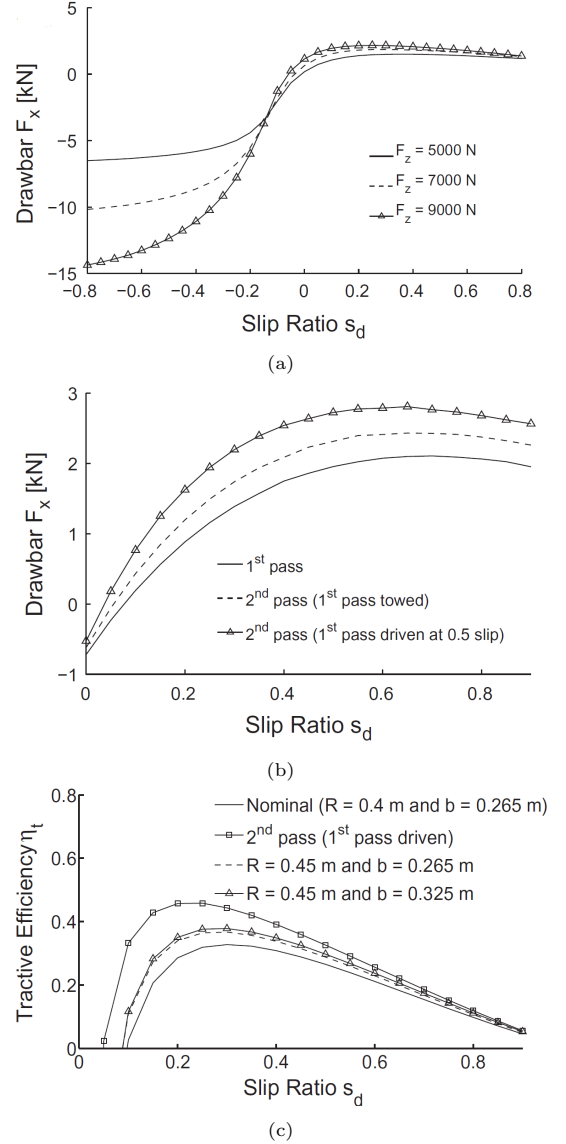


Figure 4: Provided (a-b) drawbar pull and (c) traction efficiency maps in Senatore and Sandu (2011a) of a studied off-road vehicle in terms of slip ratio, normal force and number of passes. Combining these maps, the traction efficiency is fitted to a multiparametric polynomial of order three of parameters  $\theta' = [np, F_z, F_x]$

where  $\eta_{dr}$  is efficiency of the drivetrain from energy source (i.e., battery in electric drivetrains) to contact patch of tyre including the rolling resistance.  $F_x(N)$  is the resulting longitudinal force applied to vehicle at drawbar to accelerate or pull a load (i.e., drawbar pull).  $V_x$  is the longitudinal speed of tyre ( $ms^{-1}$ ) that is same as the vehicle speed for straight motions.  $\eta_t$  is the traction efficiency of the driven tyres and is defined as ratio of the resulting drawbar power to the applied rotational power at the contact patch of tyre:

$$\eta_t(\theta') = \frac{F_x(\theta') V_x}{T_x(\theta') \omega_w} = \frac{F_x(\theta')(1 - sr(\theta')) R_{eff}}{T_x(\theta')}. \quad (14)$$

Table 1: Parameters of the soil and test vehicle.

Parameter Name	Parameter Value
Vehicle mass ( $m_s$ ) (kg)	2965
Wheelbase ( $\ell$ ) (m)	2.7
Rear axle to centre of gravity ( $bl$ ) (m)	1.9
Gearbox ratio of electric drivetrain ( $\tau_{gb}$ )	10.0
(-)	
Wheel radius ( $R_{eff}$ ) (m)	0.36
Half-track ( $d$ ) (m)	0.79
Nominal power of each electric drivetrain ( $P_{nom}$ ) (kW)	35.0
Soil type for off-road vehicle (parameters in Senatore and Sandu (2011a)) (-)	Dry sand

where  $T_x$  is driving torque at the contact patch of tyre ( $Nm$ ) due to shear stress.  $\omega_w$  is the rotational speed of the tyre ( $rad/s$ ) and  $R_{eff}$  is the effective rolling radius ( $m$ ) which is considered to be constant for efficiency calculation and equal to the smallest value around the deformed tyre.  $sr$  is the slip ratio defined as  $sr = (R_{eff}\omega_w - V_x)(R_{eff}\omega_w)^{-1}$ .

The authors in Senatore and Sandu (2011a) provided experimentally-measured drawbar pull  $F_x$  and traction efficiency  $\eta_t$  maps of driven tyres of a vehicle in terms of different slip ratios ( $sr$ ), number of passes ( $np$ ) and normal loads ( $F_z$ ). Figures 4a-4b and 4c respectively illustrate the drawbar pull and traction efficiency maps reported in Senatore and Sandu (2011a). Combining these maps, the traction efficiency is fitted to a multiparametric polynomial (15) of order three of parameters  $\theta' = [np, F_z, F_x]$ . To do the combination, the provided drawbar pull map is first fitted to a multi-parametric polynomial of order two of parameters and then is solved for slip ratio as a function of drawbar pull. The resulting parametric solution of the slip ratio is then substituted into the fitted polynomial of traction efficiency.

$$\eta_t(np, F_z, F_x) = \sum_{i=0}^3 \sum_{j=0}^{3-i} \sum_{k=0}^{3-j} a_{ijk} np^i F_z^j F_x^k. \quad (15)$$

Substituting (15) into (13) and due to the fact that  $\eta_{dr}$  depends on a parameter set of  $[V_x, a_x, a_y]$ , the resulting  $P_{loss}$  in (13) is variable in terms of  $F_x$  and depends on parameter set of  $\theta' = [V_x, F_z, a_x, a_y, np]$ . The optimal torque distribution problem (3), as a result, becomes a multi-parametric problem with  $\theta = [\tilde{F}_{ref}, \Delta M_{ref}, V_x, F_z, a_x, a_y, np]$  that can be solved off-line for  $F_x$  at different values of parameters to generate a seven-dimensional lookup table.

As an example, the problem (3) is solved for two cases by applying Theorem 2 to the left-hand-side wheels of the off-road vehicle with parameters in Table 1 Senatore and Sandu (2011a): i) the front wheel passes through the sand for the first time and the rear wheel passes exactly on the same track created by the front wheel ( $np = 0 : 1$ ); and ii) the front wheel travels on an already created track followed by the rear wheel ( $np = 1 : 2$ ). Fig. 5 summarises the simulation results for the two cases where the x-axis is the total drawbar force demand of the left-hand-side wheels.

Fig. 5a illustrates the resulting optimal distribution

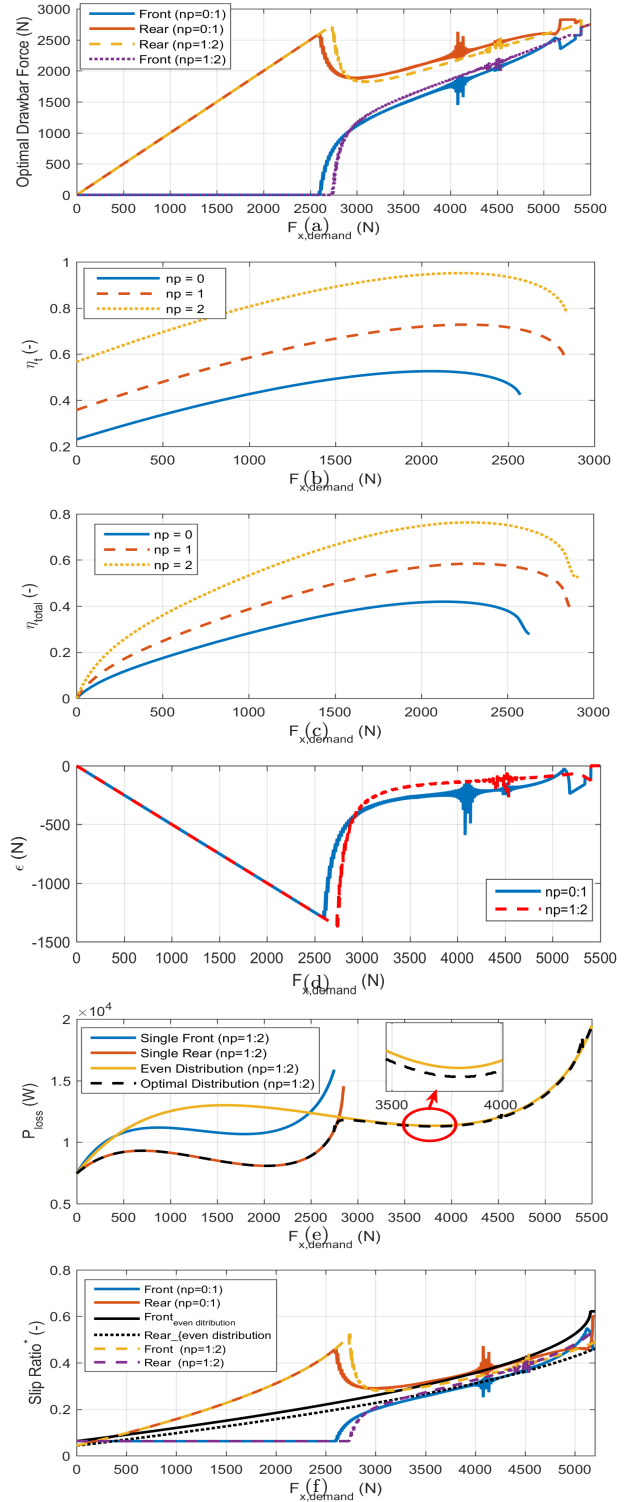


Figure 5: Simulation results of the developed optimal TDS for the off-road vehicle in Table 1 for the first and second pass(es) ( $np = 0 : 1$ ) and second and third passes ( $np = 1 : 2$ ). The calculated optimal (a) drawbar force distribution, (b) traction and (c) total efficiencies, (c) deviation from even distribution ( $\epsilon^*$ ), alongside the resulting (d) optimal power loss curves comparing to the single and even distributions, and the resulting (e) slip ratio of tyres

of the drawbar force demand between the front and rear wheels for both above cases. In both cases, the vehicle operates as rear-wheel-drive for low drawbar force demands which matches with the fact that the traction efficiency of the rear-wheels is higher due to multiple pass effects. However, once the demand exceeds a threshold (i.e., around respectively  $2600N$  and  $2720N$  for the cases (i) and (ii)), the controller splits the demands between both the front and rear wheels taking the multi-pass effect into account by applying more torque to the rear wheel. These thresholds are aligned with the traction and total efficiencies in Figs. 5b and 5c which drop sharply after the thresholds. The difference between contributions of the front and rear wheels decreases by increase in demand which matches to Fig. 4c where the traction efficiencies become similar at high slip ratios (equivalent to high applied torques). Fig. 5d depicts the corresponding calculated optimal  $\epsilon^*$  as in (9) and (10).  $\epsilon^*$  is the optimum deviation from even distribution between the front and rear wheels.

Fig. 5e shows the resulting optimal power loss curves of the above case (ii) comparing to the single and even distribution strategies. The results of case (i) show the same trends and are removed to make the figure simpler. The optimal power loss curves are generated by applying the derived optimal drawbar forces in Fig. 5a to the off-road vehicle. In Fig. 5e, it is clear that the controller tracks the minimum power losses. At high demands, the resulting power loss is lower than the one from even distribution due to the fact that the rear wheel, traveling on the compacted track, contributes more than the front wheel. In other words, the controller exploits the benefits of the multi-pass phenomenon rather than even distribution.

Fig. 5f illustrates the resulting variations of slip ratio of tyres for the above two cases. It shows that unlike the results of the prior researches (e.g. Vantsevich (2007); Senatore and Sandu (2011a)), the same slip ratios, or even distribution of the drawbar force, is not the optimal solution. It shows that at lower demands than the threshold, the optimal controller uses only one of the tyres (i.e., the rear tyre) at the region of slip ratio where the efficiency is higher. For example, Fig. 4c shows that this region is between 0.1 and 0.45 for  $n_p = 1$  which matches to the results in Fig. 5f. Once the force demand reaches to the threshold, where the traction efficiency drops, the controller engages both the tyres to maintain both the slip ratios within the region where efficiency is higher.

The glitches in all figures happen where there are multiple close sub-optimal points.

#### 4.2. Extension of the controller in Dizqah et al. (2016)

Load transformation, due to the longitudinal and lateral accelerations, changes the power loss characteristics of the drivetrains. Theorem 2 is applied to investigate the effects of the accelerations on the optimum torque distribution of electric vehicles with multiple identical drivetrains and extend the controller introduced in Dizqah et al. (2016). Based on the notations and formulation presented

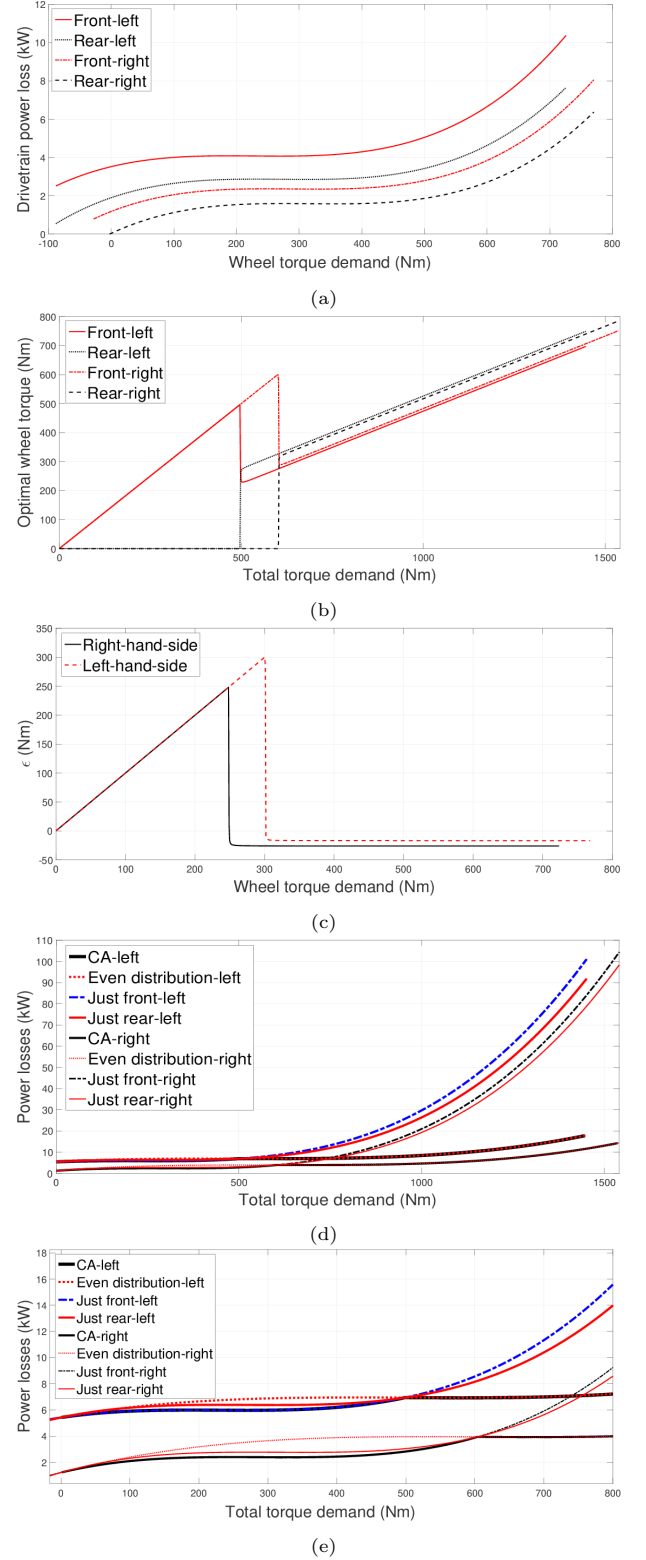


Figure 6: Applying Theorem 2 to a vehicle in Table 1 with identical drivetrains running at  $37.5km/h$  with  $a_x = 10$ ;  $a_y = -10m/s^2$ . (a) Variation of power loss curves due to acceleration; (b) calculated optimal torque distributions; (c) calculated optimal torque deviation  $\epsilon^*$ ; and (d) total power loss of the drivetrains with the introduced distribution strategy in comparison to the single-axle and the even-distribution strategies. (e) Zoomed-in version of (d) at the switching torques.

in Lenzo et al. (2017) both the rolling resistance torque and power loss vary linearly by load transformation as follow:

$$\tau_{RR}(F_z) = \tau_{RR}(F_{z0}) \frac{F_z}{F_{z0}}; \quad (16a)$$

$$P_{loss,RR}(F_z) = P_{loss,RR}(F_{z0}) \frac{F_z}{F_{z0}}. \quad (16b)$$

where  $F_z$  is the transformed load due to lateral and longitudinal accelerations and  $F_{z0}$  is the static load of each corner.

As a result, the power loss curve of each corner, in terms of the torque demand, shifts left/right and up/down by a normal load variation which is governed by equations (16a) and (16b), respectively. The resulting power loss curves depend on the values of parameters  $\theta' = [V_x, F_{z0}, a_x, a_y]$  and the optimal torque distribution problem (3) is a multi-parametric problem with  $\theta = [\bar{F}_{ref}, \Delta M_{ref}, V_x, F_{z0}, a_x, a_y]$  that can be solved off-line to generate a six-dimensional lookup table.

Fig. 6a, as an example, shows the effects of the longitudinal and lateral accelerations of  $a_x = 10$  and  $a_y = -10 \text{ ms}^{-2}$  on the power loss curves of different corners of a vehicle with identical drivetrains running at  $V = 37.5 \text{ km/h}$ . The shape of the power loss curve of each corner does not change and only shifts up/down and left/right due to the load transformation by the longitudinal and lateral accelerations. Thus, Theorem 1 is not applicable and Theorem 2 is required to calculate the optimal torque distribution among drivetrains by solving problem (10) at a set of vehicle speeds and lateral and longitudinal accelerations.

Fig. 6b illustrates the calculated optimal torque distribution between the front and rear wheels of the left- and right-hand-side of the vehicle in Table 1 at the above-given speed and accelerations. It is shown that controller employ front drivetrains for lower torque demands because of higher losses of the rear ones. Moreover, the switching torque  $\tau_{sw}$  of the right-hand-side drivetrains is larger than the left-hand-side one due to left-cornering. It is also seen that exceeding the switching torque, the controller does not distribute torque demands equivalently amongst the drivetrains but there is a difference between them which is also illustrated in Fig. 6c. Fig. 6c depicts the calculated  $\epsilon^*$  as the solution of the corresponding problem (10). Fig. 6d compares the optimal total power losses of each side of the vehicle, calculated by applying the developed strategy, to the results of: i) using only front drivetrain; ii) using only rear drivetrain; and iii) even distribution. As it shows, the resulting power loss is optimum.

#### 4.3. Optimal EMS for Hybrid Electric Vehicles

For the third case study, Theorem 2 is used to develop an energy management strategy for a compound hybrid electric powertrain in Fig. 3c where engine can either contribute to the wheels or operate in series mode. The provided 'Hybrid Electric Vehicle Input Power-Split Reference

Application' in Simulink 2018a is used as the benchmark. The reference model consists of an energy management strategy similar to the one in Toyota Prius 2010 which is a rule-based strategy implemented as a state flow. It is assumed that batteries are charged by changing the gearbox topology to series configuration and then the engine operates at its minimum fuel consumption point to charge the batteries. The performance of the built-in strategy and the proposed one are compared at a sample speed of  $70 \text{ km/h}$  and increasing slope from zero to 15 degrees (equivalent to 27%) within 30 seconds. This scenario sweeps all the torque demands at a constant speed.

To apply Theorem 2, the power loss curves of conventional drivetrain and the fuel-equivalent power loss curves of the electric drivetrain are calculated at the speed. The engine efficiency of the conventional drivetrain is usually represented as Brake Specific Fuel Consumption (BSFC) map which is defined as below Husain (2011):

$$BSFC = \frac{\dot{m}_f}{P_b} = \frac{\dot{m}_f}{2\pi N T_e}. \quad (17)$$

where  $T_e$  and  $N$  are, respectively, engine torque ( $Nm$ ) and rotational speed ( $rounds/sec$ ).  $P_b$  and  $\dot{m}_f$  are, respectively, the produced power ( $W$ ) and the corresponding fuel consumption rate ( $g/sec$ ).

The brake thermal efficiency of the engine, on the other hand, is calculated as follows:

$$\eta_{BTh} = \frac{P_b}{\dot{m}_f \cdot HHV}. \quad (18)$$

where HHV is the higher heating value of fuel Husain (2011).

Substitute (18) into (17), one gets:

$$\eta_{BTh} = \frac{1}{BSFC \cdot HHV}. \quad (19)$$

as tank-to-engine-shaft efficiency.

Therefore, for a given BSFC map and at any specific speed, the tank-to-wheels power loss curve of the drivetrain is calculated in terms of torque demand as follows:

$$P_{loss,conv} = \left( \frac{1}{\eta_{BTh} \eta_{trans}} - 1 \right) \tau_w \omega_w + P_{loss,RR}. \quad (20)$$

where  $\eta_{trans}$  is the efficiency of the transmission line from the engine shaft down to the wheels.  $P_{loss,RR}$  is the additive loss due to rolling resistance. The other losses are ignored.  $\tau_w$  and  $\omega_w$  are respectively torque and rotational speed of wheel. The gear ratios of the final drive and the gearbox at constant speed of  $70 \text{ mph}$  are respectively 3.267 and 1.360.

Similarly, the fuel-equivalent power loss curve of the electric drivetrain is calculated as follows:

$$P_{loss,elec} = \left( \frac{1}{\eta_{BTh,max} \eta_{gen} \eta_{mot} \eta_{trans}} - 1 \right) \tau_w \omega_w + P_{loss,RR}. \quad (21)$$



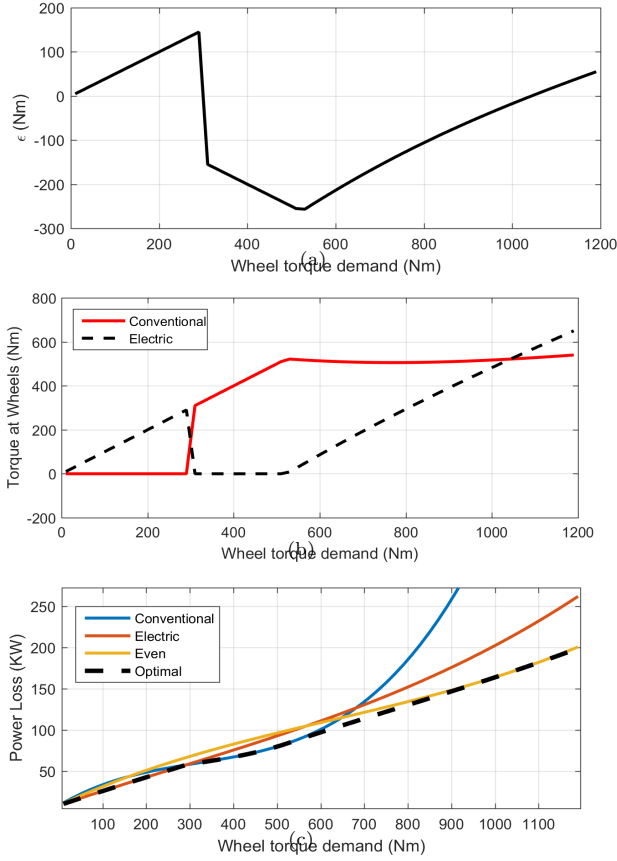


Figure 7: (a) The optimal deviation from even distribution,  $\epsilon$ , across the range of total torque demand; and the (b) optimal torque distribution between the conventional and electric drivetrains; and the resulting (c) optimum power loss curve comparing to the single-drivetrain and even distributions.

where  $\eta_{gen}$  is the efficiency of the generator at the optimum speed of the engine and is 90%. It is assumed that engine operates in series at its best fuel consumption,  $\eta_{BTh,max}$ , during charging of batteries.  $\eta_{mot}$  is efficiency of the electric motor and is provided as a map in terms of rotation speed and torque demand.

The power loss curves of the conventional and electric drivetrains of 'Hybrid Electric Vehicle Input Power-Split Reference Application' are calculated using (20) and (21) and given maps. The resulting optimal torque distribution problem (3) is a multi-parametric problem with  $\theta = [\bar{F}_{ref}, \Delta M_{ref}, V_x, F_{z0}, a_x, a_y]$  that can be solved off-line to generate a six-dimensional lookup table. Fig. 7a depicts the calculated solution of problem (10) at an example speed of  $v = 70kph = 43.5mph$ . The resulting optimum torque at wheels contributed by the conventional and electric drivetrains are illustrated in Fig. 7b for different total torque demands. The electric drivetrain supplies all the torque demand less than  $240Nm$  where the conventional drivetrain solely contributes after. The torque demand larger than  $520Nm$  are provided with both the drivetrains at different rates depending on the amount of torque demand.

Fig. 7c illustrates the resulting optimal power loss of

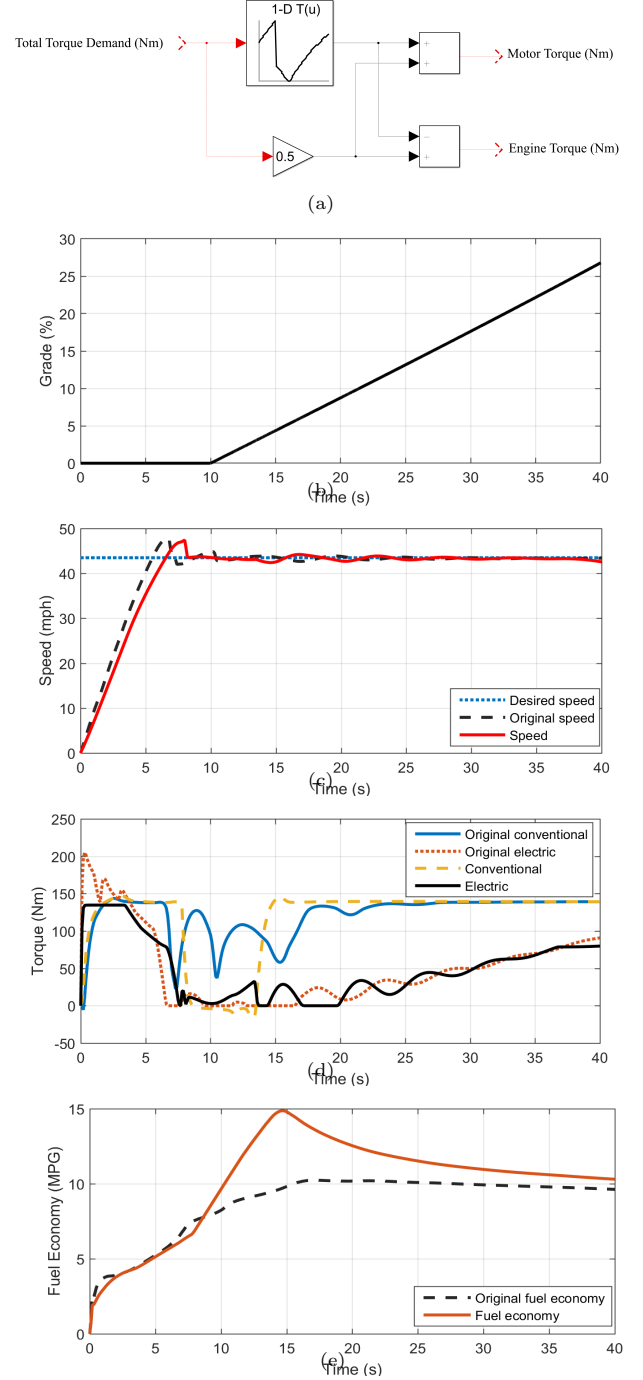


Figure 8: (a) A lookup table implementation of the developed energy management strategy for the compound hybrid powertrain in Fig. 3c at a sample speed of  $70kph = 43.4mph$  and increasing road grade in (b); and the performance comparison of the developed strategy to the original one in SIMULINK 'Hybrid Electric Vehicle Input Power-Split Reference Application' example in terms of (c) speed regulation, (d) torque distribution between the hybrid powertrain and (e) the resulting fuel economy.

the powertrain comparing to the even distribution and single-drivetrain cases. The even distribution and single-drivetrain are respectively the cases when torque demand

evenly splits between the drivetrains or is supplied solely by one of the drivetrains. Fig. 7c shows that the calculated torque distribution in Fig. 7b minimises total power loss of the powertrain.

The calculated optimal  $\epsilon$ , i.e., deviation from even distribution, in Fig. 7a is stored in a lookup table within the model as the energy management strategy. Fig. 8a shows an implementation of the strategy which is obviously very simple and quick. Performance of the developed energy management strategy is compared with the built-in strategy at constant speed of 70kph and road grade changes as in Fig. 8b. The scenario sweeps all torque demands at the constant speed. Fig. 8c indicates that the vehicle speed starts from zero with both strategies and reaches to 70kph (equivalent to 43.4mph) and stay constant afterwards. The resulting torque distribution generated by the developed strategy comparing to the one from the original strategy in the model are depicted in Fig. 8d. Both of the strategies use the two conventional and electric drivetrains at the beginning of the scenario when the car accelerates and needs high torque. They also employs both the drivetrains, though at different rates, during the second half of the scenario when the road grade is large and substantial torque is needed. The main difference is at low and middle torques, i.e., after reaching the target speed and during the moderate grades, where strategies operate differently. The original strategy uses the electric drivetrain to assist the conventional one while the developed strategy turns off the engine during low torque demands (between 7 – 18s) and turns off the electric motor during middle torques (between 18 – 20s). The fuel economy comparison is provided in Fig. 8e which shows slight improvement by the developed strategy at the end of the scenario while it is much simpler to implement and faster to operate.

## 5. Conclusions

This paper introduces an algorithm to solve the optimal torque distribution problem offline, in terms of energy consumption, for both on- and off-road vehicles with multiple drivetrains. The drivetrains have been represented with their total power loss curves which have been then integrated into the introduced theorem to dynamically calculate the optimal contribution of each drivetrain. In this paper, for the first time the original multi-parametric non-convex problem (non-convex mp-NLP) has been converted to a multi-parametric quadratic programming (mp-QP) problem. The resulting mp-QP can be solved online having the instantaneous values of parameters or can be solved offline using multi-parametric optimisation tools.

Unlike prior researches, the introduced control strategy is not limited to the monotonically increasing and convex power loss curves and can be applied to any type of drivetrains. The simulation results indicate that the developed control strategies improve energy consumption comparing to the well-known single-axle and even distribution counterparts. Moreover, it indicates that unlike the

general understanding, even when the drivetrains are exactly the same the even-distribution (for on-road vehicles) and equal-slip-ratios (for off-road vehicles) strategies are only applicable to the very high torque demands where the power loss curves become convex. Non-convexity of the power loss curves at the low torque demands, on the other hand, causes the single-wheel or less-balanced distribution strategies become the optimal ones for a wide range of the operating points.

The introduced theorem provides a systematic approach to formulate and solve the problem offline to generate small-sized multi-dimensional lookup tables for fast real-time implementation of the optimal control strategy.

## References

- Chen, Y., Wang, J., 2014a. Adaptive energy-efficient control allocation for planar motion control of over-actuated electric ground vehicles. *IEEE Transactions on Control Systems Technology* 22, 1362–1373. doi:10.1109/TCST.2013.2287560.
- Chen, Y., Wang, J., 2014b. Design and experimental evaluations on energy efficient control allocation methods for overactuated electric vehicles: Longitudinal motion case. *IEEE/ASME Transactions on Mechatronics* 19, 538–548. doi:10.1109/TMECH.2013.2249591.
- Dizqah, A.M., Lenzo, B., Sornioti, A., Gruber, P., Fallah, S., Smet, J.D., 2016. A fast and parametric torque distribution strategy for four-wheel-drive energy-efficient electric vehicles. *IEEE Transactions on Industrial Electronics* 63, 4367–4376. doi:10.1109/TIE.2016.2540584.
- Domínguez, L.F., Narciso, D.A., Pistikopoulos, E.N., 2010. Recent advances in multiparametric nonlinear programming. *Computers & Chemical Engineering* 34, 707 – 716. URL: <http://www.sciencedirect.com/science/article/pii/S0098135409002634>, doi:<https://doi.org/10.1016/j.compchemeng.2009.10.012>. selected Paper of Symposium ESCAPE 19, June 14–17, 2009, Krakow, Poland.
- Grancharova, A., Johansen, T.A., 2012. Multi-parametric Programming. Springer Berlin Heidelberg, Berlin, Heidelberg. chapter 1. pp. 1–37. URL: [https://doi.org/10.1007/978-3-642-28780-0\\_1](https://doi.org/10.1007/978-3-642-28780-0_1), doi:10.1007/978-3-642-28780-0\_1.
- Huang, Y., Wang, H., Khajepour, A., Li, B., Ji, J., Zhao, K., Hu, C., 2018. A review of power management strategies and component sizing methods for hybrid vehicles. *Renewable and Sustainable Energy Reviews* 96, 132 – 144. URL: <http://www.sciencedirect.com/science/article/pii/S1364032118305240>, doi:<https://doi.org/10.1016/j.rser.2018.07.020>.
- Husain, I., 2011. Electric and Hybrid Vehicles: Design Fundamentals, Second Edition. Taylor & Francis. URL: [https://books.google.co.uk/books?id=7AAWH\\_63HuAC](https://books.google.co.uk/books?id=7AAWH_63HuAC).
- Lenzo, B., Filippis, G.D., Dizqah, A.M., Sornioti, A., Gruber, P., Fallah, S., Nijs, W.D., 2017. Torque distribution strategies for energy-efficient electric vehicles with multiple drivetrains. *ASME Journal of Dynamic Systems, Measurement, and Control* 139, 121004–121004–13. doi:10.1115/1.4037003.
- Senatore, C., Sandu, C., 2011a. Off-road tire modeling and the multi-pass effect for vehicle dynamics simulation. *Journal of Terramechanics* 48, 265 – 276. URL: <http://www.sciencedirect.com/science/article/pii/S0022489811000401>, doi:<https://doi.org/10.1016/j.jterra.2011.06.006>.
- Senatore, C., Sandu, C., 2011b. Torque distribution influence on tractive efficiency and mobility of off-road wheeled vehicles. *Journal of Terramechanics* 48, 372 – 383. URL: <http://www.sciencedirect.com/science/article/pii/S0022489811000425>, doi:<https://doi.org/10.1016/j.jterra.2011.06.008>.

- Suzuki, Y., Kano, Y., Abe, M., 2014. A study on tyre force distribution controls for full drive-by-wire electric vehicle. *Vehicle System Dynamics* 52, 235–250. URL: <https://doi.org/10.1080/00423114.2014.894198>, doi:10.1080/00423114.2014.894198, arXiv:<https://doi.org/10.1080/00423114.2014.894198>.
- Taheri, S., Sandu, C., Taheri, S., Pinto, E., Gorsich, D., 2015. A technical survey on terramechanics models for tire-terrain interaction used in modeling and simulation of wheeled vehicles. *Journal of Terramechanics* 57, 1 – 22. URL: <http://www.sciencedirect.com/science/article/pii/S0022489814000664>, doi:<https://doi.org/10.1016/j.jterra.2014.08.003>.
- Tang, Y., 2010. Dual motor drive and control system for an electric vehicle. Google Patents, US Patent App. 12/782,413.
- Vantsevich, V.V., 2007. Multi-wheel drive vehicle energy/fuel efficiency and traction performance: Objective function analysis. *Journal of Terramechanics* 44, 239 – 253. URL: <http://www.sciencedirect.com/science/article/pii/S0022489807000171>, doi:<https://doi.org/10.1016/j.jterra.2007.03.003>.
- Wang, H., Huang, Y., Khajepour, A., 2018. Cyber-physical control for energy management of off-road vehicles with hybrid energy storage systems. *IEEE/ASME Transactions on Mechatronics* 23, 2609–2618. doi:10.1109/TMECH.2018.2832019.